Pergamon

Bioorganic & Medicinal Chemistry 6 (1998) 1811–1819

BIOORGANIC & MEDICINAL CHEMISTRY

Molecular Modeling Studies of the Binding Modes of Aldose Reductase Inhibitors at the Active Site of Human Aldose Reductase

Yong S. Lee,* Zhou Chen and Peter F. Kador

National Eye Institute, National Institutes of Health, Bethesda, MD 20892, USA

Received 15 December 1997; accepted 12 May 1998

Abstract—Molecular modeling studies using the CHARMM method have been conducted to study the binding modes of aldose reductase inhibitors at the active site of aldose reductase. The energy minimized structures of aldose reductase with six structurally diverse inhibitors (spirofluorene-9,5′-imidazolidine-2′,4′-dione (**1**), 9-fluoreneacetic acid (**2**), AL1576 (**3**), 2,7-difluoro-9-fluoreneacetic acid (**4**), FK366 (**5**), and Epalrestat (**9**)) indicate that the side chains of Tyr48, His110, and Trp111 can form numerous hydrogen bonds with either the carboxylate or the hydantoin group of the inhibitors while the side chains of Trp20, Trp111, and Phe122 are positioned to form aromatic–aromatic interactions. Of the three residues (Tyr 48, His 110, and Trp 111) that can form hydrogen bonds with the ionized portion of aldose reductase inhibitors, protonated His110 appears to play an important role in directing charged inhibitors to bind at the active site through charge interaction. Based on the binding mode of the inhibitors and their observed inhibitory activities, pharmacophore requirements for aldose reductase inhibitors are discussed. Published by Elsevier Science Ltd.

Introduction

Aldose reductase (E.C. 1.1.1.21; ALR2) is an enzyme in the polyol pathway which utilizes the coenzyme NADPH to reduce the aldehyde form of glucose to sorbitol. Aldose reductase has been linked to several diabetic complications.[1–3] Animal studies have demonstrated that aldose reductase inhibitors (ARIs), when administered from the onset of hyperglycemia, prevent the progression of polyol accumulation-linked complications in a dose-dependent manner.[3,4] The feasibility that inhibition of aldose reductase provides a pharmacologically direct treatment for diabetic complications that is independent of the control of blood sugar levels has spurred the development of structurally diverse ARIs.[2,3,5]

Despite their structural diversity, common electronic and steric features among ARIs were identified through molecular orbital calculations, structure–activity relationship studies, and computer modeling.[6–8] Co-crystallization of aldose reductase with NADP(H) cofactor and the ARI zopolrestat has shown that zopolrestat binds to the catalytic site[9,10] of aldose reductase, which comprises Tyr48, His110, Cys298, and the nicotinamide ring of NADP(H) as well as Trp20, Trp111 Phe122, and Leu300. Compounds possessing an anionic group such as citrate, glucose-6-phosphate, and cacodylate have also been observed to cocrystallize at the catalytic site.[11] In contrast to the crystallographic finding, an alternative inhibitor binding site on aldose reductase that is independent of the substrate binding site had been proposed based on the affinity labeling studies and a non- or uncompetitive behavior of ARIs in the NADPH-dependent reduction of glucose to sorbitol.[12] However, more evidence favoring the active site as the inhibitor binding site has emerged recently. These include crystal structures that have shown that the ARIs tolrestat and sorbinil bind to the active site of porcine aldose reductase[13] and aldehyde reductase[14] as well as molecular modeling work carried out at the active site of aldose reductase.[15,16]

ARIs primarily contain either a carboxylate or an ionizable hydantoin group[17–20] suggesting that both the

Key words: Aldose reductase inhibitors; hydrogen bond; charge interaction; aromatic–aromatic interaction; pharmacophore requirements.

*Corresponding author: Tel.: 301 496 8548; Fax: 301 402 2399; E-mail: yongslee@helix.nih.gov

0968-0896/98/$—see front matter Published by Elsevier Science Ltd.
PII: S0968-0896(98)00139-4

carboxylate and the hydantoin group can bind in a similar manner to aldose reductase. This possibility was examined in previous molecular modeling studies on ARIs by superimposing ARIs containing an ionizable carboxylate (e.g. **2**) or tetrazole group onto spirofluorene-9,5′-imidazolidine-2′,4′-dione (**1**).[8] In this study, it was proposed that a negative charge residing in the vicinity of the 2′-oxygen atom of the hydantoin ring participates in binding interactions. The crystal structures of aldose reductase complexed with NADP(H) and zopolrestat reveal a salt-bridge formation between the carboxylate of zopolrestat and His110.[9,10] This crystallographic finding suggests that the positively charged His110 not only interacts with the carboxyl anion of ARIs but also with the negatively charged hydantoin ring of ARIs through charge interaction.

In the present study, molecular modeling of six structurally diverse ARIs (**1–5** and **9**) has been carried out at the active site of aldose reductase to probe the charge interaction between the ionizable group (e.g. carboxylate or hydantoin) of the ARIs and the positively charged His110. An attempt was also made to correlate the binding mode of these structurally diverse inhibitors

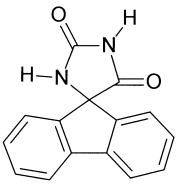

1

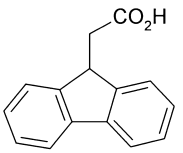

2

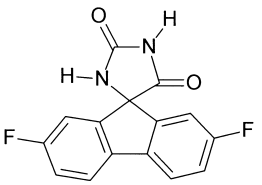

3

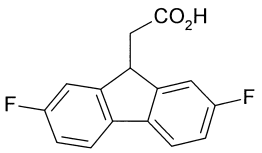

4

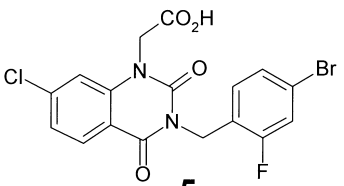

5

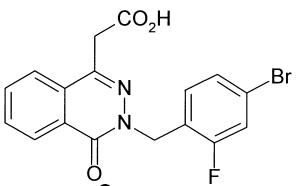

6

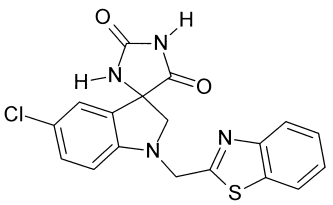

7

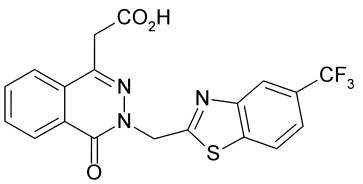

8

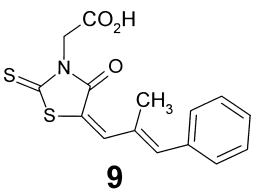

9

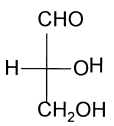

10

to observed inhibitory activity. In addition, the binding mode of these inhibitors at the active site has been compared to that of D-glyceraldehyde (**10**) substrate.

Methodology

The coordinates of human aldose reductase complexed with NADP(H) and crystal water (1ADS)[21] were obtained from the Brookhaven Protein Data Bank. Hydrogens were added to the amino acid residues of human aldose reductase using the HBUILD routine of CHARMM.[22] ARIs (**1–5** and **9**) were manually docked into the active site of aldose reductase complexed with $NADP^+$ so that the ionized group could form hydrogen bonding interactions with Tyr48 and His110 while the fluorene ring or heterocyclic portion of the inhibitors was stacked against Trp20. The carbonyl oxygen of D-glyceraldehyde (**10**) was positioned within the distance of hydrogen bonding interactions with Tyr48 and His110 at the active site of aldose reductase complexed with NADPH. Crystal water molecules and citrate[11] overlapping inhibitors or D-glyceraldehyde at the active site were removed. Single point energy calculations with the 6-31G* basis set[23] were conducted to assign partial charges to $NADP^+$ NADPH, inhibitors and D-glyceraldehyde. Compounds **2–5** and **9** were treated as negatively charged whereas compound **1** was treated as both negatively charged and neutral. With the exception of His110, all His residues were treated as neutral with hydrogen assigned to the Nδ1 of neutral histidine. His110 was treated as positively charged based on the crystallographic evidence that the carboxylate of zopolrestat is salt-linked to the Nε2 hydrogen of His110.[9,10] All Asp and Glu residues were assumed to be negatively charged while Arg and Lys were positively charged. The complex of both ALR2-$NADP^+$-ARI and ALR2-NADPH-D-glyceraldehyde were hydrated by placing it into a sphere of water molecules, and subsequently deleting all water molecules except those with oxygens at least 2.5 Å away from the complex. After hydration, all water molecules located more than 4.5 Å away from the complex were also removed. The geometry of the hydrated complex was then energy minimized by CHARMM using an all-atom parameter set.[24] The hydrated complex with a harmonic positional restraint of $k = 1.0$ on ARL2-$NADP^+$-ARI or ARL2-NADPH-D-glyceraldehyde was minimized for the initial 1000 steps using the steepest descent method and then the subsequent 1000 steps with the adopted basis Newton–Raphson (ABNR) method to allow the water molecules to optimize relative to the protein. The hydrated complex was further minimized without restraints using ABNR method until the energy gradient fell below 0.01 kcal/mol/Å. Energy minimizations were performed with a constant dielectric constant ($\varepsilon = 1$). Electrostatic force was treated with the force switch method with a switching range of 8–12 Å. van der Waals forces were calculated using the shift method with a cutoff of 12 Å. All calculations by CHARMM were performed on a cluster of HP-735 workstations.

Results and Discussion

Binding mode of spirofluorene-9,5′-imidazolidine-2′,4′-dione and 9-fluoreneacetic acid

The optimized structure of spirofluorene-9,5′-imidazolidine-2′,4′-dione (**1**) at the active site (Fig. 1) indicates that the negatively charged hydantoin ring forms a number of hydrogen bonds with Tyr48, His110, and Trp111. The Nε2 hydrogen of His110 is hydrogen bonded to the 4′ oxygen and 3′ nitrogen while the hydroxyl of Tyr48 and the Nε1 hydrogen of Trp111 form hydrogen bonds with the 2′ oxygen and 4′ oxygen, respectively. The hydrogen bonds formed in Figure 1 are in good agreement with reported crystallographic results between the hydantoin ring of sorbinil and the amino acid residues at the active site of porcine aldose reductase.[13] The modeling of neutral compound **1** at the active site (Fig. 2) results in the loss of hydrogen bonds between the Nε2 hydrogen of His 110 and the hydantoin. This is due to a steric repulsion between the Nε2 hydrogen of His110 and the hydrogen on the 3′ nitrogen of the hydantoin. Figure 2 indicates that the hydrogen on the 3′-nitrogen on the hydantoin forms hydrogen bonds with the amide oxygen of the $NADP^+$ and the Nε2 atom of His110. This hydrogen bonding pattern, however, is not supported by the crystallographic finding.[13] The closer resemblance of the hydrogen bonding interactions in Figure 1 to those reported in the crystal structure, therefore, suggests that hydantoins at physiological pH are negatively charged as proposed in the superposition study.[8]

The carboxylate of 9-fluoreneacetic acid (**2**) at the active site (Fig. 3) also forms a number of hydrogen bonds with Tyr48, His110, and Trp111. As illustrated in Figure 3, the Nε2 hydrogen of His110 is hydrogen-bonded to both of the carboxylate oxygen atoms while the hydroxyl of Tyr48 and the Nε1 hydrogen of Trp111 form a hydrogen bond to each of the two carboxylate oxygens. The hydrogen bonds formed in Figure 3 are in good agreement with reported crystallographic results between the carboxylate of zopolrestat and the amino acid residues at the active site of aldose reductase.[10,11]

Based on the crystallographic findings and kinetic work, it has been suggested that the coenzyme $NADP^+$ provides a charge interaction to the negatively charged group of ARIs in the ternary complex.[11,26] However, it

remains controversial whether ARIs preferentially bind to the binary complex of AR-NADPH[27] or AR-$NADP^+$.[28] Irrespective of the oxidation state of the cofactor, both the crystallographic findings[9,10] and the hydrogen bonding patterns illustrated in Figures 1 and 3 suggest that protonated His110 rather than $NADP^+$ primarily provides the charge interaction to the negatively charged group of ARIs. Furthermore, because of its ability to form a salt-bridge, protonated His110 is likely to play a more important role than neutral His110 with the Nε2 hydrogen in directing charged inhibitors to bind at the active site of aldose reductase.

Comparison of the inhibition data (IC_{50}) in Table 1 of compounds **1** and **2** for human aldose reductase illustrates that the hydantoin containing compound **1** is a

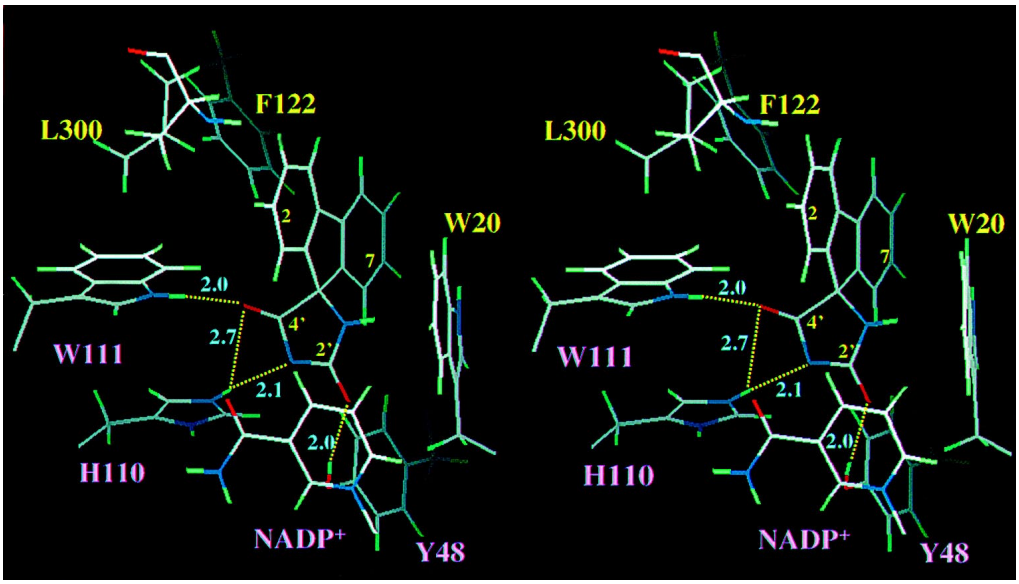

Figure 1. Stereoview of the CHARMM energy minimized structure of aldose reductase complexed with negatively charged spirofluorene-9,5′-imidazolidine-2′,4′-dione **1**. Dotted lines indicate the hydrogen bonding interactions (< 3.0 Å). All figures except 8 were prepared by using Quanta 3.3.

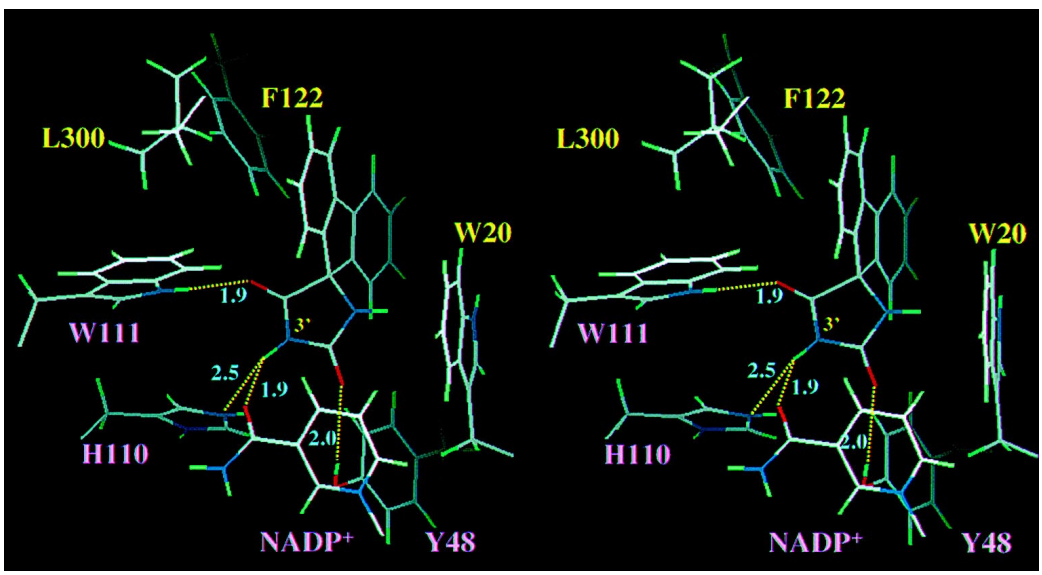

Figure 2. Stereoview of the CHARMM energy minimized structure of aldose reductase complexed with neutral spirofluorene-9,5′-imidazolidine-2′,4′-dione **1**.

75-fold better inhibitor than the carboxylate containing compound **2**. Since these two compounds possess a fused fluorene ring as a common backbone, the stronger inhibitory activity of compound **1** than compound **2** may arise from the hydantoin group that can form stronger hydrogen bonding interactions than the carboxylate group. The rigidity of the hydantoin ring compared to the flexible carboxylate group may orient the heteroatoms on the hydantoin for more favorable hydrogen bonding interactions with Tyr48, His110, and Trp111. As illustrated in Figure 1, three of the five heteroatoms on the hydantoin ring can form hydrogen bonds. Figure 1 further suggests that the presence of a bulky group at either the 1′ or 3′ nitrogen position on the hydantoin is likely to cause a severe disruption of the hydrogen bonding interactions. This may explain the more than 100-fold decrease in inhibitory activity of the spirohydantoin derivatives with methyl substitution at either the 1′ or 3′ nitrogen position as compared to the spirohydantoin derivative without substitution.[29]

The energy minimized structures (Figs 1 and 3) indicate that the side chains of Trp20, Trp111, and Phe122 are all positioned for van der Waals interaction with the fluorene ring of compounds **1** and **2**. Most notably, the fluorene ring of compounds **1** and **2** is sandwiched between Trp20 and Phe122 suggesting that the fluorene ring interacts with Trp20 and Phe122 through aromatic–aromatic interactions.[30,31] It has been known that hydrophobic interactions enhance inhibitor binding. However, a weak inhibitory activity (IC_{50}, 10^{-3}–10^{-4} M) of variety of aliphatic acids such as octanoic acid and keto acids[32] indicates that the aromatic–aromatic interactions play a more important role in enhancing the inhibitory activity of ARIs. The significance of the aromatic–aromatic interactions in binding inhibitors to aldose reductase is further supported by mutation studies,[28] which reported the decreased inhibitory activity of ARIs such as AL1576 by more than 500-fold upon the replacement of Trp20 of human aldose reductase by alanine.

Table 1. Activity of ARIs

Compd	IC_{50} (10^{-6} M)
1	0.49
2	37
3	0.064
4	0.16
5	0.17
6	0.042
7	0.037[a]
8	0.025[a]
9	14

[a]Ref 20; IC_{50} values for compounds **1–6** and **9** were determined in a reaction mixture consisted of 10 mU of recombinant human muscle aldose reductase, 0.3 mM of NADPH, 10 mM of DL-glyceraldehyde, and 0.1 M of phosphate buffer, pH 6.2.

Based on the binding mode shown in Figures 1 and 3, the observed IC_{50} values for compounds **1** and **2** in 10^{-5} to 10^{-7} molar range can be attributed to a combination of hydrogen bonding and aromatic–aromatic interactions. The binding mode of difluoro substituted analogs **3** and **4** are essentially the same as those of the corresponding unfluorinated compounds **1** and **2** except that the 2 fluorine atom of compound **3** forms a hydrogen

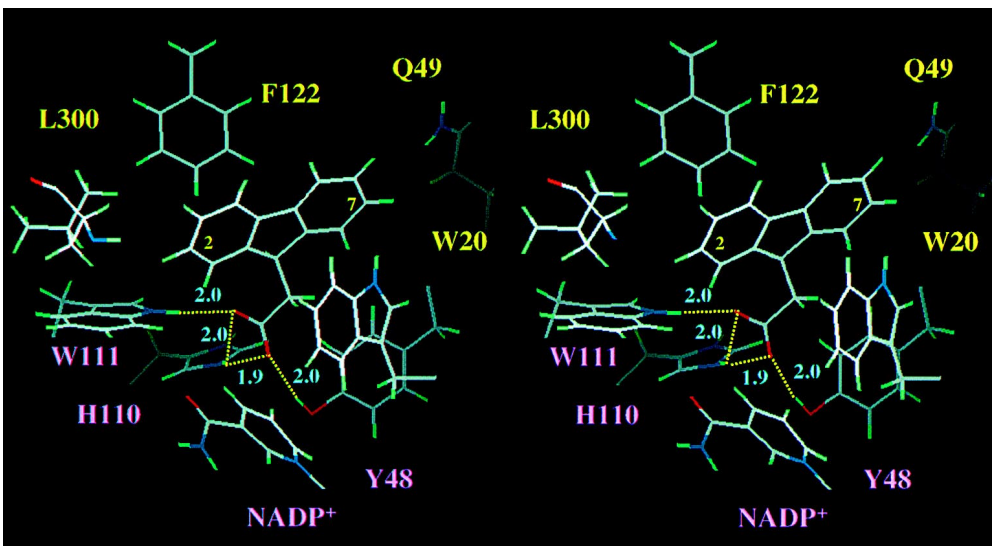

Figure 3. Stereoview of the CHARMM energy minimized structure of aldose reductase complexed with 9-fluoreneacetic acid **2**.

bond with the main chain of N-H of Leu300 (Fig. 1) while the 2 and 7 fluorine atoms of compound **4** hydrogen-bond to the main chain of N-H of Leu300 and the NH_2 group of Gln49 (Fig. 3), respectively. Thus, the enhanced inhibitory activity of compounds **3** and **4** by 8- to 230-fold relative to the respective unfluorinated compounds **1** and **2** can be attributed to the increase in both hydrogen bonding and aromatic–aromatic interactions due to the presence of two fluorine atoms.

Binding mode of FK366

The topology of compounds (FK366 (**5**), Ponalrestat (**6**) and the spirohydantoin (**7**)) is comparable to zopolrestat (**8**) in that they possess an ionizable group and a heterocyclic backbone with a pendent aromatic group. This suggests that the binding modes of compounds **5–7** to aldose reductase are likely to resemble those of zopolrestat crystallized at the active site of human aldose reductase.[10] To test this premise, FK366 was docked onto the active site of aldose reductase based on the published description of the binding mode of zopolrestat.[10,11] Despite the large geometrical perturbation introduced when the pendent aromatic ring is inserted between Trp111 and Leu300, the optimized structure (Fig. 4) shows that the carboxylate of FK366 still forms multiple hydrogen bonds with the side chains of Tyr48, His110, and Trp111. The two carbonyls of the heterocyclic backbone of FK366 can be also seen to hydrogen-bond to Cys298 and a water molecule. Figure 4 also displays that the heterocyclic backbone of FK366 is positioned between Trp20 and Phe122 to form aromatic–aromatic interactions. In addition to the hydrogen bonding and the aromatic–aromatic interactions which are comparable to those shown in Figures 1 and 3, the pendent aromatic group intercalated between Trp111 and Leu300 may provide an additional aromatic–aromatic interactions in enhancing the binding of FK366 to aldose reductase. Pendent aromatic groups such as benzothiazole attached to the heterocyclic backbone of ARIs have been earlier recognized as another pharmacophore group of ARIs that binds strongly to amino acid residues of aldose reductase at some distance away from the site which binds to acidic groups.[20] The inhibitory activity of a pyridazinone acetic acid containing the pendent group benzothiazole was reported ca. 80-fold stronger for bovine lens aldose reductase than the unsubstituted pyridazinone acetic acid.[16] This finding further supports the role of the additional aromatic–aromatic interaction in enhancing the binding affinity of ARIs. The binding mode of FK366 in Figure 4 is essentially the same as that of zopolrestat crystallized at the active site of aldose reductase. Molecular modeling studies[16] on a pyridazinone acetic acid containing a benzothiazole group have also reported a binding mode comparable to that shown in Figure 4. Because of the similarity in topology, compounds **6** and **7** are expected to bind to aldose reductase like FK366 and zopolrestat. Accordingly, the observed IC_{50} values for compounds **5–8** in 10^{-7} to 10^{-8} molar range (Table 1) can be attributed to a combination of hydrogen bonding interactions and two distinct aromatic–aromatic interactions. Furthermore, inhibitors with pendent groups (e.g. **5–8**) have been known to display greater selectivity by ca. 100- to 1000-fold for inhibiting aldose reductase over aldehyde reductase while inhibitors without the pendent group (e.g. **1–4**) display comparable inhibition for both enzymes.[33,34]

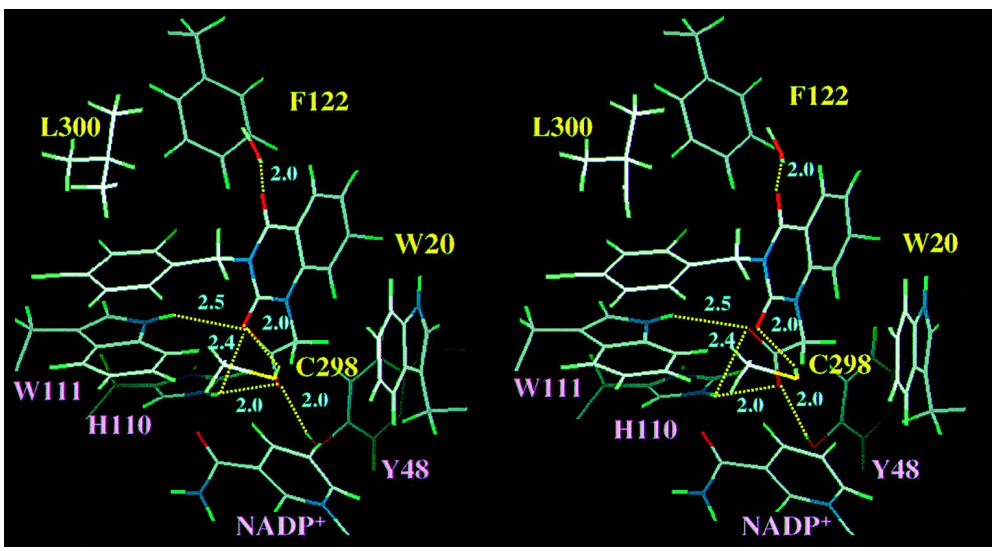

Figure 4. Stereoview of the CHARMM energy minimized structure of aldose reductase complexed with FK366 **5**.

This suggests that the pendent group not only enhances the binding affinity of ARIs but also has an ability to differentiate aldose reductase from aldehyde reductase.

Binding mode of Epalrestat

The side chain of Epalrestat (**9**) cannot readily be superimposed onto that of compounds **5–8** because of a double bond linkage between the heterocyclic backbone and the side chain. Manual docking of Epalrestat onto the active site suggests that accommodation of the side chain of Epalrestat is better when it is oriented toward Phe122 rather than between Trp111 and Leu300. This is in agreement with the superposition study,[8] which has shown that the spatial orientation of the side chain of Epalrestat differs from that of FK366 and Ponalrestat. The energy minimized structure (Fig. 5) displays that the carboxylate group of Epalrestat hydrogen-bonds to Tyr48, His110, and Trp111 while Cys298 and a water molecule hydrogen-bond to the sulfur atoms of the heterocyclic backbone. The phenyl portion of Epalrestat may form aromatic–aromatic interaction with Phe122. Epalrestat, however, does not have an aromatic backbone that can interact with Trp20, Trp111, and Phe122.

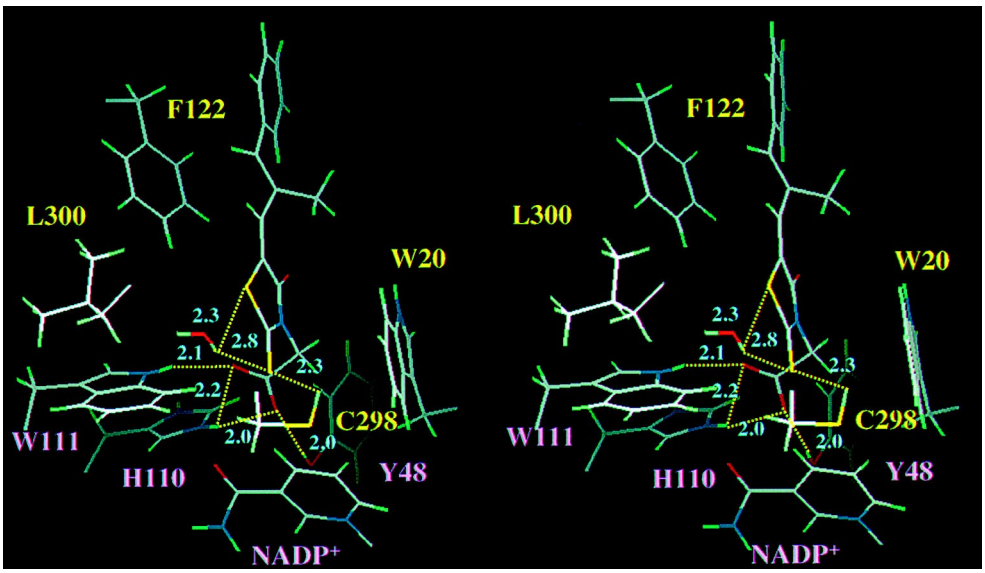

Figure 5. Stereoview of the CHARMM energy minimized structure of aldose reductase complexed with Epalrestat **9**.

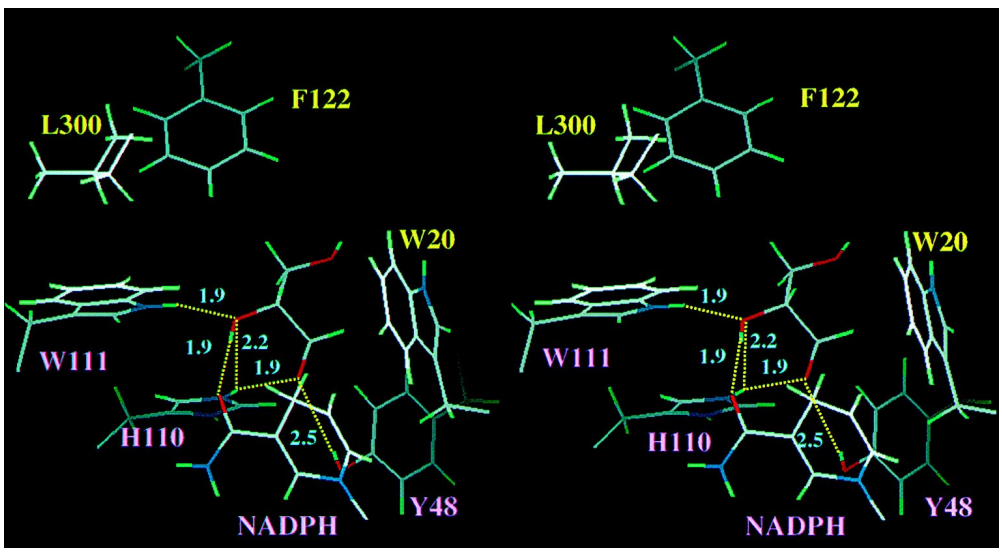

Figure 6. Stereoview of the CHARMM energy minimized structure of aldose reductase complexed with D-glyceraldehyde **10**.

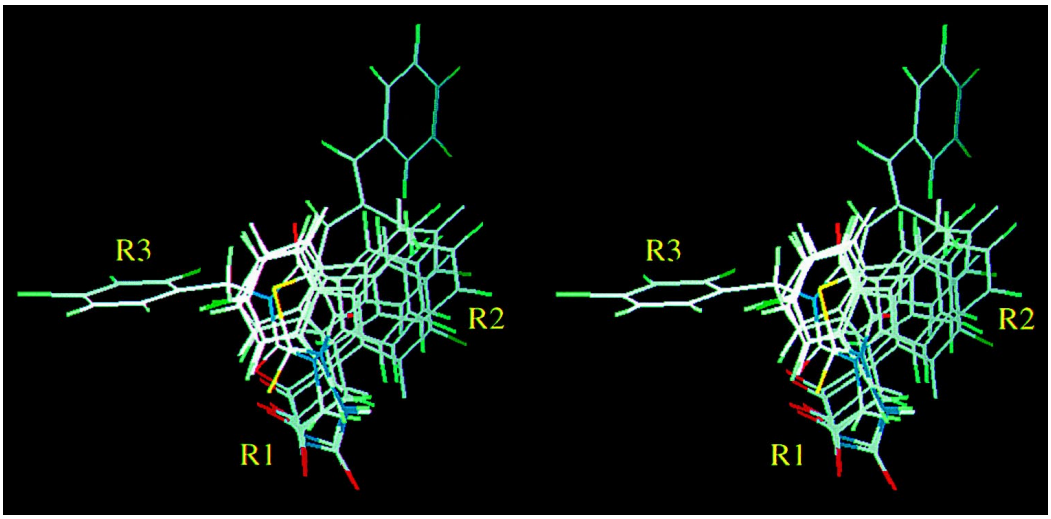

Figure 7. Stereoview of the superposition of the energy minimized structures of **1–5** and **9** at the active site of aldose reductase. R1 and R2 denote the spatial position of the ionized group and the aromatic backbone, respectively. R3 denotes the spatial position of the side chain of FK366 **5**.

The absence of proper aromatic–aromatic interactions may explain why the inhibitory activity of Epalrestat for human aldose reductase is ca. 80- to 330-fold weaker than compounds **3–6**.

Binding mode of D-glyceraldehyde

The energy minimized structure of D-glyceraldehyde (**10**) at the active site (Fig. 6) displays that the substrate carbonyl hydrogen bonds with both His110 and Tyr48 while the 2′-hydroxyl group forms hydrogen bonds with His110, Trp111, and the amide oxygen of NADPH. These multiple hydrogen bonds are comparable to those formed by the carboxylate or the hydantoin of ARIs as shown in Figures 1 and 3–5. Moreover, the charge interaction between His110 and the carboxylate or the hydantoin appears to resemble the charge interaction developing between His110 and the substrate carbonyl oxygen at the transition state.[35] Therefore, ARIs containing a carboxylate or a hydantoin group can be considered as pseudo transition state analogs of the aldehyde substrate.

Pharmacophores of ARIs

Figure 7, depicting the superposition of the energy minimized inhibitors **1–5** and **9** at the active site of aldose reductase, illustrates that both the ionized portion (R1) of **1–5** and **9** and the aromatic portion (R2) of **1–5** overlap well in space. It also shows the spatial orientation of the side chain (R3) with respect to the aromatic portion. By combining the spatial position of R1, R2, and R3 of the inhibitors of **1–5** and **9** with their binding modes and inhibitory activities, the pharmacophore

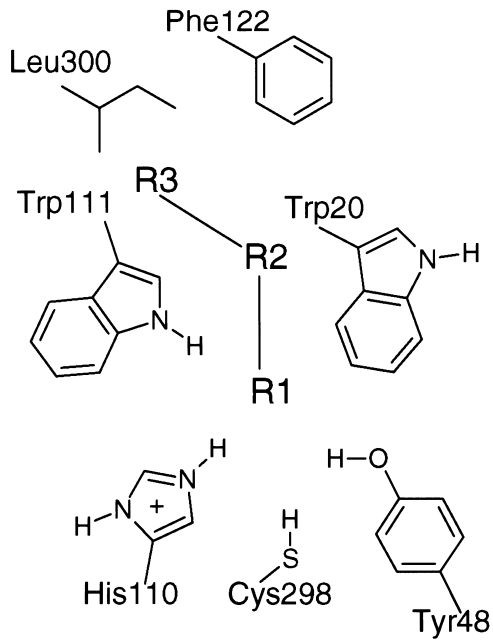

Figure 8. Schematic diagram depicting the pharmacophores of ARIs.

requirements of ARI can be depicted as follows (Fig. 8): An ionized portion (R1) of ARI forms hydrogen bonding interactions with the side chains of Tyr48, His110, and Trp111 while an aromatic portion (R2) can form aromatic–aromatic interactions with the side chains of Trp20, Trp111, and Phe122. The aromatic portion can also form hydrogen bonding interactions with Cys298 and the main chain of N-H of Leu300. A side chain (R3)

such as benzothiazole can intercalate between Trp111 and Leu300 to further improve aromatic–aromatic interactions. In terms of inhibitory activity as measured by IC_{50}, ARIs having a hydrogen-bonding R1 group and a proper R2 group can have IC_{50} values in the range of 10^{-7} to 10^{-8} molar as evidenced by the IC_{50} values of compounds **1, 3**, and **4**. For ca. 100-fold or more increased inhibitory specificity for aldose reductase over aldehyde reductase and IC_{50}s in the range of 10^{-8} molar, ARIs require an intercalating R3 on top of both hydrogen bonding R1 and aromatic R2 groups.

Conclusion

The present molecular modeling studies based on the crystallographic findings suggest that His110 plays a crucial role in directing charged inhibitors containing either a carboxylate or an ionizable hydantoin group to the active site of aldose reductase by providing charge interaction. Charged ARIs have been suggested to bind aldose reductase as pseudo transition state analogs of the aldehyde substrate. The combination of hydrogen bonding and aromatic–aromatic interactions has been attributed to play a major role in enhancing the binding affinity of ARIs.

Acknowledgements

Useful discussions with Dr. Katsumi Sugiyama are gratefully acknowledged.

References and Notes

1. Kinoshita, J. H. *Am. J. Ophthalmol.* **1986**, 685.

2. Dvornik, D. In *Aldose Reductase Inhibition*; Porte, D., Ed.; McGraw-Hill: New York, 1987; Chapter 5.

3. Kador, P. F. *Med. Res. Rev.* **1988**, *8*, 325.

4. Kador, P. F.; Akagi, Y.; Terubayashi, H.; Wyman, M.; Kinoshita, J. H. *Arch. Ophthalmol.* **1988**, *106*, 1109.

5. Humber, L. In *Aldose Reductase Inhibition*; Porte, D., Ed.; McGraw-Hill: New York, 1987; Chapter 4.

6. Kador, P. F.; Sharpless, N. E. *Mol. Pharmacol.* **1983**, *24*, 521.

7. Kador, P. F.; Sharpless, N. E.; Kinoshita J. H. *J. Med. Chem.* **1985**, *28*, 841.

8. Lee, Y. S.; Pearstein R.; Kador P. F. *J. Med. Chem.* **1994**, *37*, 781.

9. Wilson, D. K.; Tarle I.; Petrash, J. M.; Quiocho, F. A. *Proc. Natl. Acad Sci. U. S. A.* **1993**, *90*, 9847.

10. Wilson, D. K.; Nakano T.; Petrash, J. M.; Quiocho, F. A. *Biochemistry* **1995**, *34* 14323.

11. Harrison, D. H.; Bohren, K. M.; Ringe D.; Petsko, G. A.; Gabbay, K. H. *Biochemistry* **1994**, *33* 2011.

12. Kador, P. F.; Lee, Y. S.; Rodriguez L.; Sato S.; Malik A. B.; Ghany Y. S.; Miller D. D. *Bioorg. Med. Chem.* **1995**, *3*, 1313.

13. Urzhumtsev, A.; Tete-Favier, F.; Mitschler, A.; Barbanton, J.; Barth, P.; Urzhumtseva, L.; Bielmann, J. F.; Podjarny, A. D.; Moras, D. *Structure* **1997**, *5*, 601.

14. El-Kabbani, O.; Carper, D.; McGowan, M. H.; Devedjiev, Y.; Rees-Milton, K. J.; Flynn, T. G. *Proteins: Struct. Func. Genet.* **1997**, *29*, 186.

15. Constantino, L.; Rastelli, G.; Vescovini, K.; Cignarella, G.; Vianello, P.; Del Corso, A.; Cappiello, M.; Mura, U.; Barloco, D. *J. Med. Chem.* **1996**, *39*, 4396.

16. Rastelli, G.; Vianello, P.; Barlocco, D.; Constantino, L.; Del Corso, A.; Cignarella, G.; Mura, U. *Bioorg. Med. Chem. Lett.* **1997**, *7*, 1897.

17. DeRuiter, J.; Brubaker, A. N.; Whitmer, W. L.; Stein, J. L. *J. Med. Chem.* **1986**, *29*, 2024.

18. Ellingboe, J.; Alessi, T.; Millen, J.; Sredy, J.; King, A.; Prusiewicz C.; Guzzo F.; VanEngen D.; Bagli J. *J. Med. Chem.* **1990**, *33*, 2892.

19. Malamas, M. S.; Millen, J. *J. Med. Chem.* **1991**, *34*, 1492.

20. Mylari, B. L.; Larson, E. R.; Beyer, T. A.; Zembrowski, W. J.; Aldinger, C. E.; Dee, M. F; Siegel, T. W.; Singleton, D. H. *J. Med. Chem.* **1991**, *34*, 108.

21. Wilson, D. K.; Bohren, K. M.; Gabbay, K. H.; Quiocho, F. A. *Science* **1992**, *257*, 81.

22. Brooks, B. R.; Bruccoleri, R. E.; Olafson, B. D.; States, D. J.; Swaminathan, S.; Karplus, M. *J. Comput. Chem.* **1983**, *4*, 187.

23. Frisch, M. J.; Trucks, G. W.; Schlegel, H. B.; Gill, P. M. W; Johnson, B. G.; Robb, M. A.; Cheeseman, J. R.; Keith T.; Petersson, G. A.; Montgomery, J. A.; Raghavachari, K.; Al-Laham, M. A.; Zakrzewski, V. G.; Ortiz, J. V.; Foresman, J. B.; Cioslowski, J.; Stefanov, B. B.; Nanayakkara, A.; Challacombe, M.; Peng C. Y.; Ayala Y.; Chen W.; Wong M. W.; Anders, J. L.; Replogle, E. S.; Gomperts, R.; Martin, R. L.; Fox, D. J.; Binkley, J. S.; Defrees, D. J.; Baker J.; Stewart, J. P.; Head-Gordon, M.; Gonzalez, C.; Pople J. A.: Gaussian 94, Revision C. 2, Gaussian, Inc., Pittsburgh PA, 1995.

24. Molecular Simulation Inc., Parameter file for CHARMm version 22, 1992, Waltham, MA.

25. Steinbach, P. J.; Brooks, B. R. *J. Comput. Chem.* **1994**, *15*, 667.

26. Grimshaw, C. E.; Bohren, K. M.; Lai, C. J.; Gabbay, K. H. *Biochemistry* **1995**, *34* 14374.

27. Nakano, T.; Petrash, J. M. *Biochemistry* **1996**, *35*, 11196.

28. Ehrig, T.; Bohren, K. M.; Prendergast, F. G.; Gabbay, K. H. *Biochemistry* **1994**, *33*, 7157.

29. Yamagishi, M.; Yamada, Y.; Ozaki, K.; Assao, M.; Shimizu, R.; Suzuki, M.; Matsumoto, M.; Matsuoko, Y.; Matsumoto, K. *J. Med. Chem.* **1992**, *35*, 2085.

30. Burley, S. K.; Petsko, G. A. *Science* **1985**, *229*, 23.

31. Sapse, A. M.; Schweitzer B. S.; Dicker, A. P.; Bertiono, J. R.; Frecer, V. *Int. J. Pep. Prot. Res.* **1992**, *39*, 18.

32. Hayman, S.; Kinoshita, J. H. *J. Biol. Chem.* **1965**, *240*, 877.

33. Sato, S.; Kador, P. F. *J. Diab. Comp.* **1993**, *7*, 179.

34. Sato, S.; Kador, P. F. *Biochem. Pharmacol.* **1990**, *40*, 1033.

35. Lee, Y. S.; Milan H.; Brooks, B. R.; Kador P. F. *Biophys. Chem.* **1998**, *70*, 203.